Elemental Phosphorus Stabilized Ni_2P for Efficient Electrooxidation of 5-Hydroxymethylfurfural to 2,5-Furandicarboxylic Acid

Zihan Ning,[a] Xiaojun Cao,[b] Fengyun Liu,[b] Guofeng Zhang,*[a] Yibo Yan,[c] Yinghui Liu,[a] Xiantao Chang,[d] Jinghai Zhang,[e] Shahzad Murtaza,[f] Rifat Jawaria,[f] Aziz Bakhtiyarovich Ibragimov,[g] Dianxiang Xing,[a] Yan Tian,[a] Zunqi Liu,[c] Baoying Li,*[a] Jianbin Chen*[a,c]

[a] School of Chemistry and Chemical Engineering, Qilu University of Technology (Shandong Academy of Sciences), Jinan, 250353, P. R. China

[b] Qilu Pharmaceutical Co., Ltd, Jinan, 250100, P. R. China

[c] Chemistry and Chemical Engineering College, Xinjiang Agricultural University, Urumqi 830052, P. R. China

[d] Shandong Dongchen New Technology Co., Ltd., 250200, P. R. China

[e] Shandong Hua Fluorochemical Co., Ltd., 250204, P. R. China

[f] Institute of Chemistry, Khwaja Fareed University of Engineering and Information Technology, Rahim Yar Khan, 64200, Pakistan.

[g] Institute of General and Inorganic Chemistry of Uzbekistan Academy of Sciences, M.Ulugbek Str., 77A, Tashkent 700170, Uzbekistan.

* Corresponding author: jchen@qlu.edu.cn

Experimental Section

1.1 Synthesis of catalysts

1.1.1 Hydrothermal treatment of rough red phosphorus

5 g rough red phosphorus was grinded with 5 mL deionized water to pulverize too large bulks, which was then transferred into a 100 mL Teflon-lined stainless-steel autoclave and heated to 200 °C for a period of 12 h. After that, the red phosphorus through hydrothermal treatment was separated by rinsing to abandon minor bulks or particles with distilled water and ethanol for several times, and dried in a vacuum at 60 °C overnight. The obtained hydrothermal processed product maintained the phase of amorphous red phosphorus (Fig. S1).

1.1.2 Preparation of porous Ni_2P or P/ Ni_2P

238 mg $NiCl_2.6H_2O$ and various amounts of hydrothermal-treated red phosphorus was directly added into a 20 mL ptfe liner, which was then filled with triethanolamine up to 80 % of the total volume and transferred into the stainless-steel autoclave for tightening. After that, the autoclave was

heated to 130 °C for a period of 16 h. After the accomplishment of the reaction, the autoclave was cooled down to room temperature naturally and the product was separated by centrifugation, washed with distilled water and ethanol several times, and dried in a vacuum at 60 °C overnight.

1.2 Characterization

X-ray diffraction (XRD) measurements were performed on a Bruker D8 Focus Diffraction system with Cu Ka radiation (λ = 0.15418 nm) at V = 40 kV and I = 40 mA. Transmission electron microscope (TEM) images were recorded on a Tecnai G220STwin transmission electron microscope at an accelerating voltage of 120 kV. The chemical states of the elements were determined by X-ray photoelectron spectroscopy (XPS) using Kratos Axis Ultra DLD multi-technique.

1.3 Electrochemical Measurements

The fabrication procedure of working electrode was as follow: 3 mg of dried catalyst was dispersed in 0.96 mL of a mixture of deionized water and ethanol (Vol_{water}: $Vol_{ethanol}$ = 1: 3). Then, 40 μL of Nafion solution (5 wt%, Sigma-Aldrich) was added followed by an ultrasonic process for about 25 min, obtaining a homogenous ink. 200 μL of the ink was then drop-cast onto a clean 1 cm × 1 cm carbon fiber paper (CFP) (catalyst loading: 0.6 mg cm^{-2}), which was air-dried at room temperature to obtain the catalyst film. The CFP coated with catalyst, a graphite rod and Hg/HgO electrode were used as working, counter and reference electrodes, respectively.

All voltages were calibrated against the reversible hydrogen electrode (RHE). The oxygen evolution reaction (OER) performance was evaluated in a H-type cell with 1.0 M KOH as the electrolyte. For the 5-hydroxymethylfurfural oxidation reaction (HMFOR) test, 5 mM of 5-hydroxymethylfurfural (HMF) was added to 10 mL of 1.0 M KOH solution. Linear sweep voltammetry (LSV) curves were obtained at a scan rate of 5 m $V \cdot s^{-1}$. The electrochemical specific surface area (ECSA) of the electrode was determined by means of the double-layer capacitance (C_{dl}). Cyclic voltammetry measurements were conducted in the non-Faradaic region ranging from 0.76 V to 0.96 V at scan rates of 20, 40, 60, 80, 100 and 120 $mV \cdot s^{-1}$ in an electrolyte consisting of 10 mL of 1.0 M KOH mixed with 5 mM HMF.

1.4 Product analysis

The electrooxidation of HMF was conducted via chronoamperometry at a voltage of 1.45 V vs. RHE in an H-type electrolytic cell at room temperature for 5 h. Both the anodic and cathodic

chambers were loaded with 10 mL of 1 M KOH solution containing 5 mM HMF for the measurement. Afterwards, 200 μL of the electrolyte from the anodic chamber was diluted to a total volume of 2 mL using ultrapure water. High-performance liquid chromatography (HPLC) analysis was then performed at room temperature with an ultraviolet-visible (UV-Vis) detector set at a wavelength of 280 nm, employing a BIO-RAD Aminex HPX-87H column with dimensions of 7.8 mm × 300 mm. Quantitative analysis of the products was conducted via the external standard method based on the pure intermediates of HMF, HMFCA, DFF, FFCA, and FDCA.

The conversion rate of HMF, yield of FDCA, selectivity of FDCA, and Faradaic efficiency (FE) were calculated using the following formulas:

$$\text{Conversion (\%)} = \frac{\text{mol of HMFconsumed}}{\text{mol of initial HMF}} \times 100\%$$

$$\text{Yield (\%)} = \frac{\text{mol of FDCA formed}}{\text{mol of initial HMF}} \times 100$$

$$\text{Selectivity (\%)} = \frac{\text{mol of produced FDCA}}{\text{mol of consumed HMF}} \times 100\%$$

$$\text{FE (\%)} = \frac{n \times F \times mol\ of\ FDCA\ formed}{total\ charge\ passed} \times 100\%$$

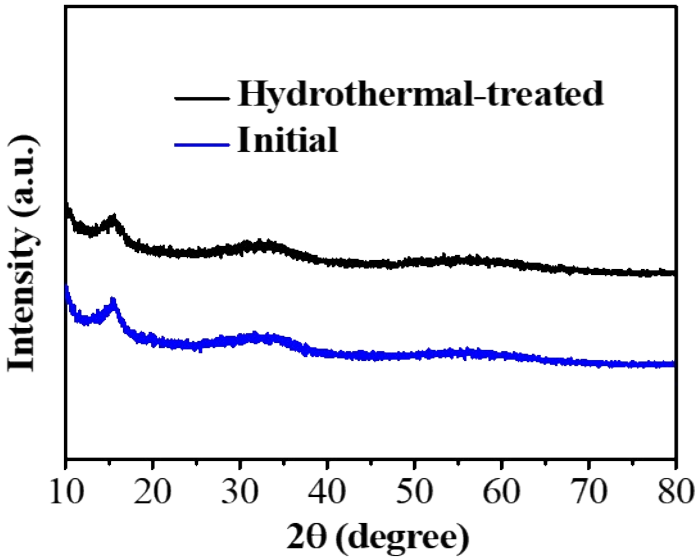

Fig. S1 XRD patterns of initial and hydrothermal-treated red phosphorous.

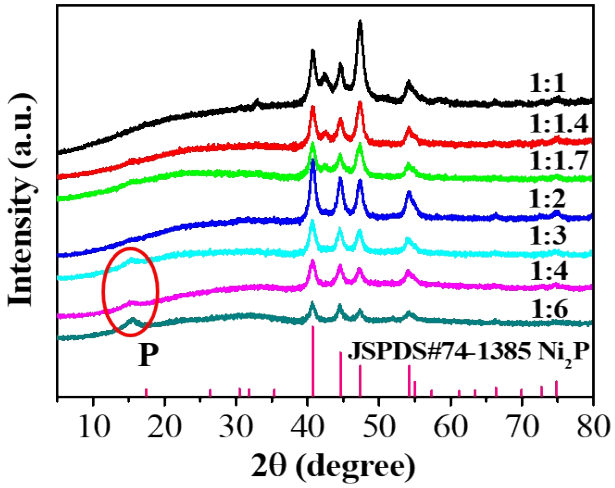

Fig S2. XRD patterns of Ni_2P samples obtained with different molar ratio of $NiCl_2$:P from 1:1 to 1:6.

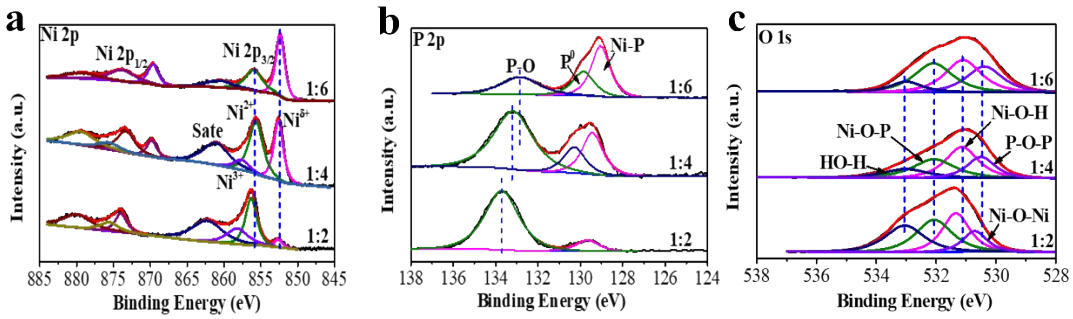

Fig. S3 a) Ni 2p, b) P 2p and c) O 1s high-resolution XPS spectra for P@Ni_2P-2, P@Ni_2P-4 and P@Ni_2P-6.

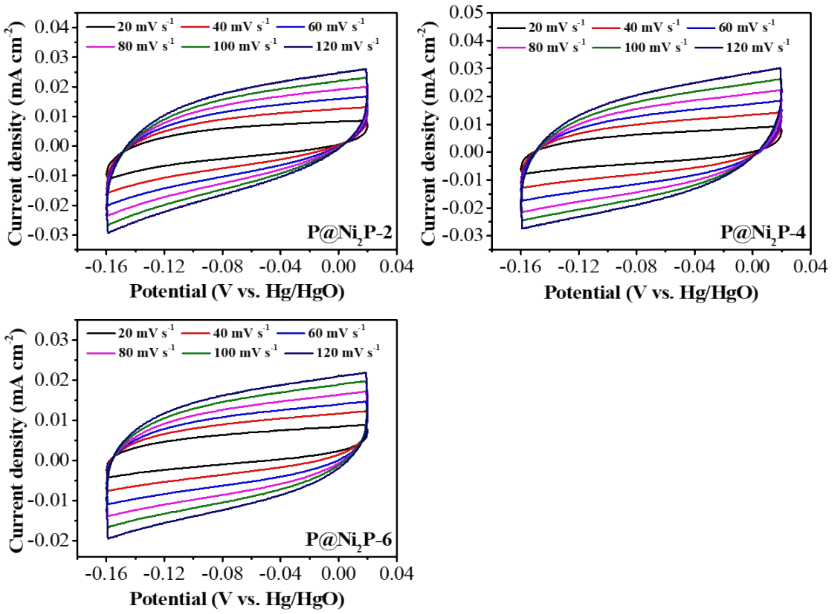

Fig. S4 CV curves for P@Ni_2P-2, P@Ni_2P-4 and P@Ni_2P-6 obtained at series scan rates from 20 to 120 mV s^{-1} in 1 M KOH + 5 mM HM.

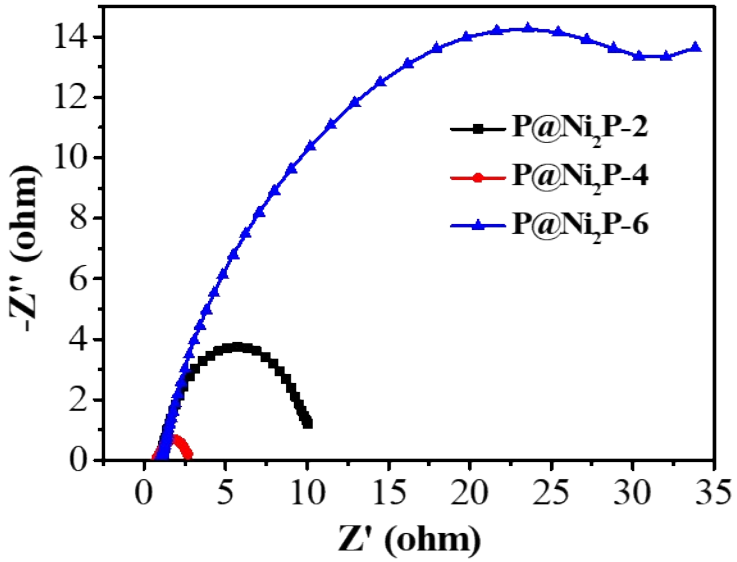

Fig. S5 Nyquist plots of P@Ni_2P-2, P@Ni_2P-4 and P@Ni_2P-6 in 1 M KOH with 5 mM HMF.

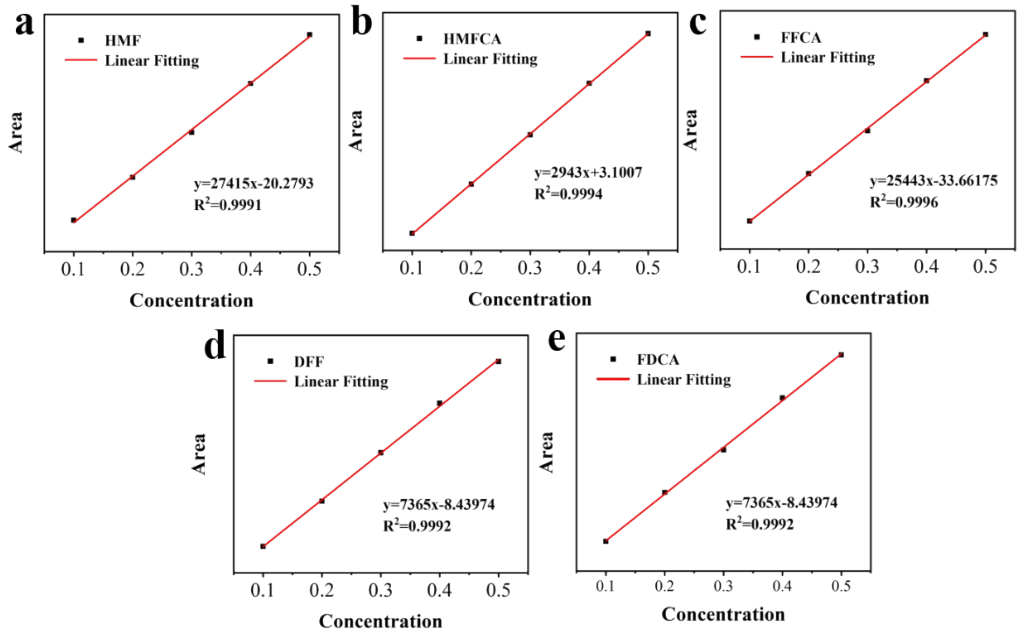

Fig. S6 Standard curves determined by HPLC for: a) HMF, b) HMFCA, c) FFCA, d) DFF and e) FDCA.

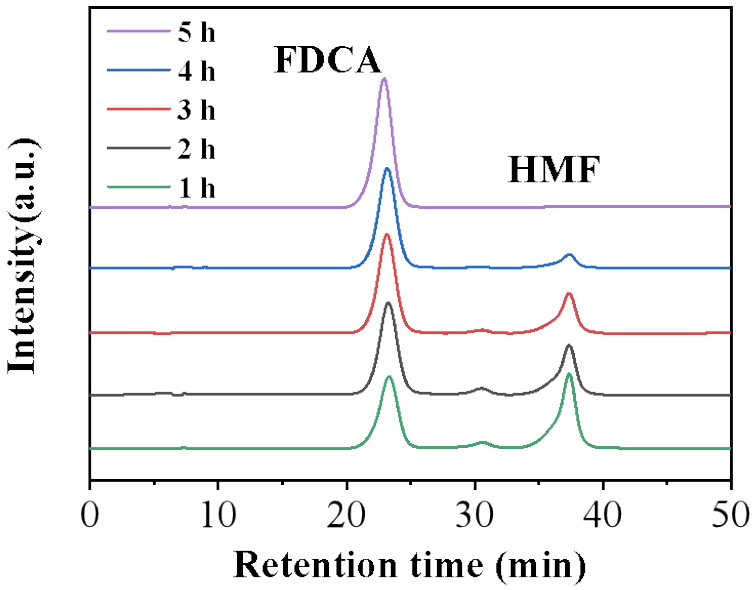

Fig. S7 HPLC spectra of various products at different reaction times after the electrochemical oxidation reaction of HMF (mobile phase: 5 mM sulfuric acid aqueous solution; flow rate: 1.0 mL min^{-1}; temperature: 35 °C).

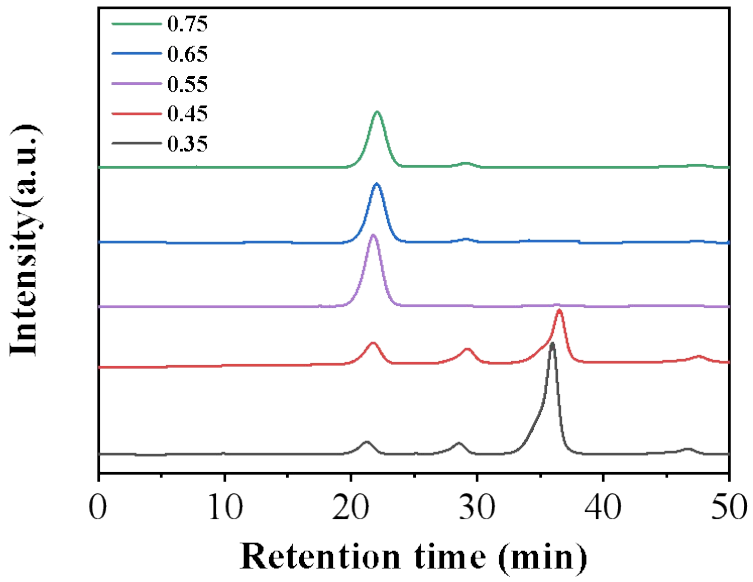

Fig. S8 HPLC of HMFOR at different voltages (vs. Hg/Hg O).

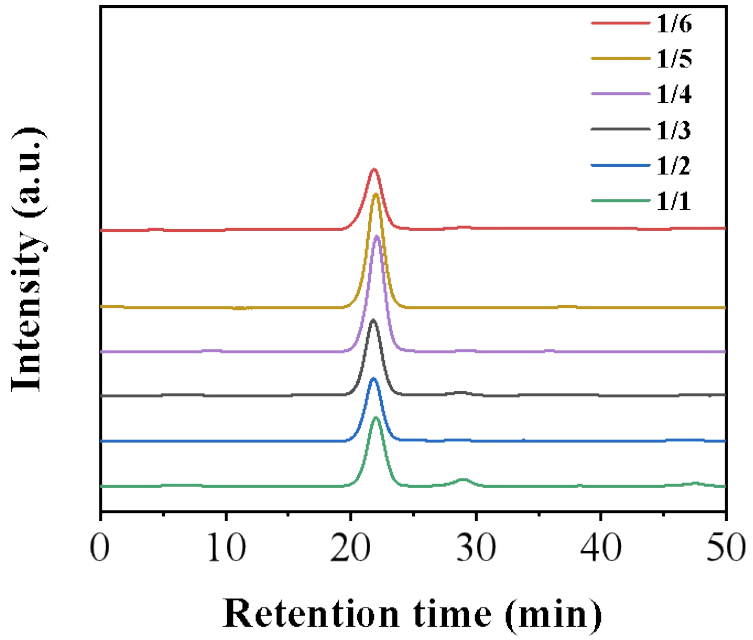

Fig. S9 HPLC of HMFOR over various catalysts with molar ratio of $NiCl_2$:P from 1:1 to 1:6.

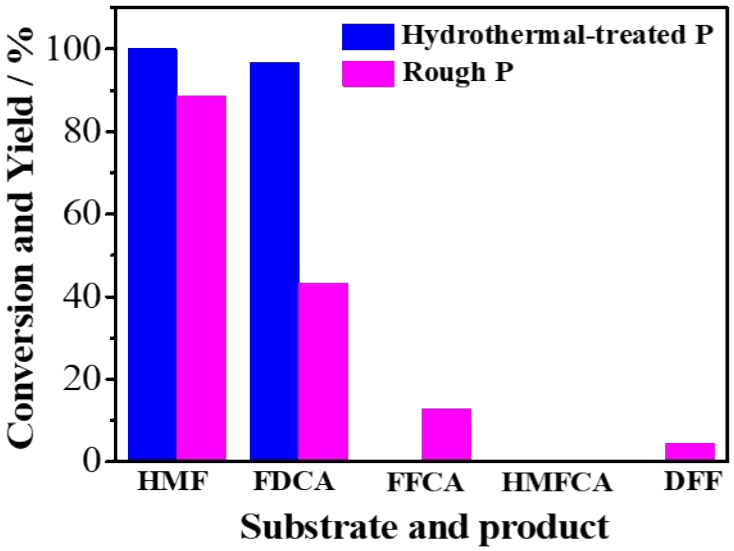

Fig. S10 Reaction results for HMFOR catalyzed by catalysts fabricated using hydrothermal-treated and rough red phosphorous.

As we can see, the conversion rate and selectivity have both significantly lowered when using rough red phosphorus to replace the hydrothermal-treated red phosphorus.

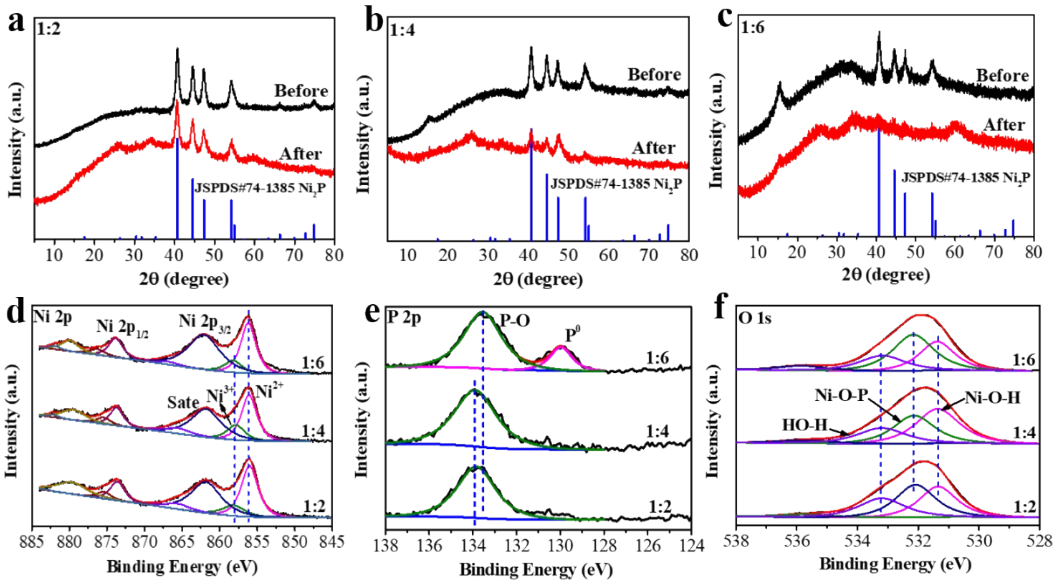

Fig. S11 XRD patterns before and after HMFOR for: a) P@Ni_2P-2, b) P@Ni_2P-4 and c) P@Ni_2P-6. d) Ni 2p, e) P 2p and f O 1s high-resolution XPS spectra after HMFOR for P@Ni_2P-2, P@Ni_2P-4 and P@Ni_2P-6.

The broad diffraction peak found around 2θ=25° was ascribed to the carbon fiber substrate (Figure S12).

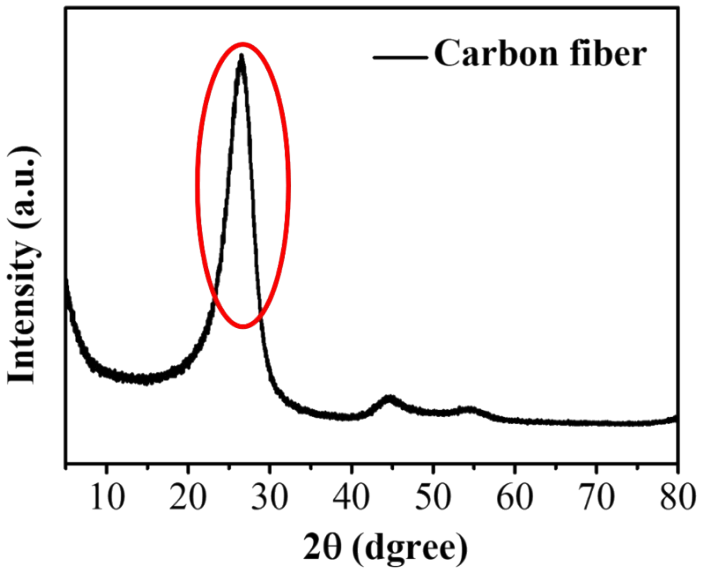

Fig. S12 XRD pattern of pure carbon fiber.

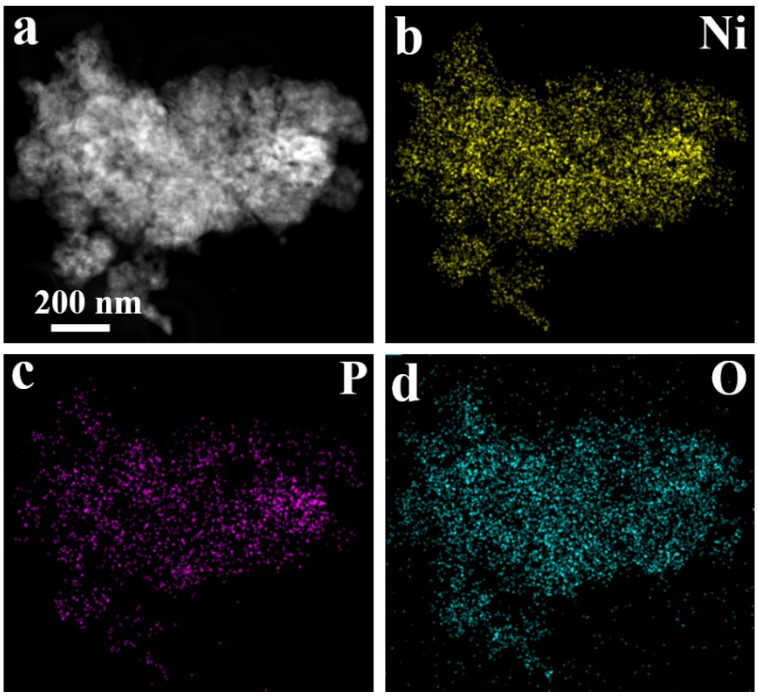

Fig. S13 HAADF-STEM image and corresponding elemental mapping images for P@Ni_2P-2 after HMFOR.

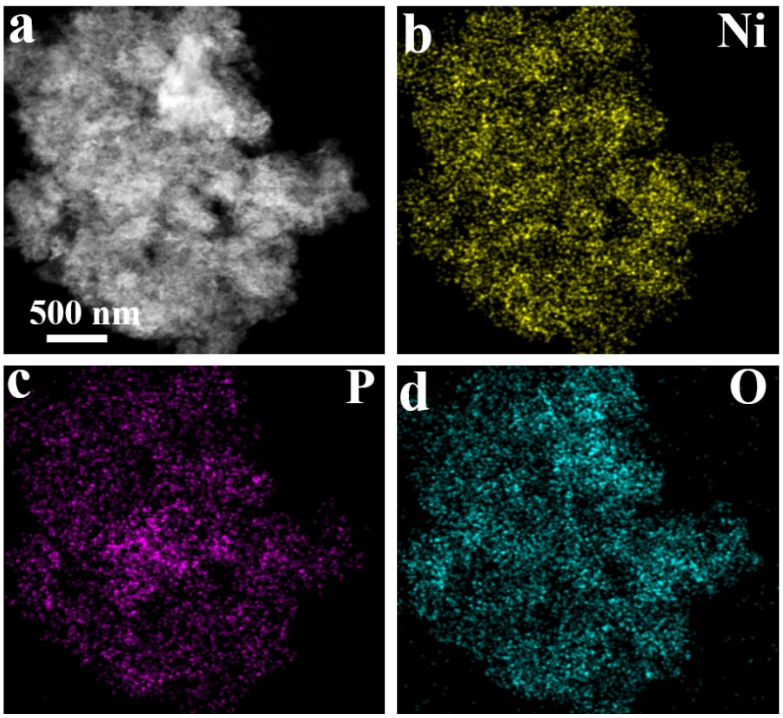

Fig. S14 HAADF-STEM image and corresponding elemental mapping images for P@Ni_2P-4 after HMFOR.

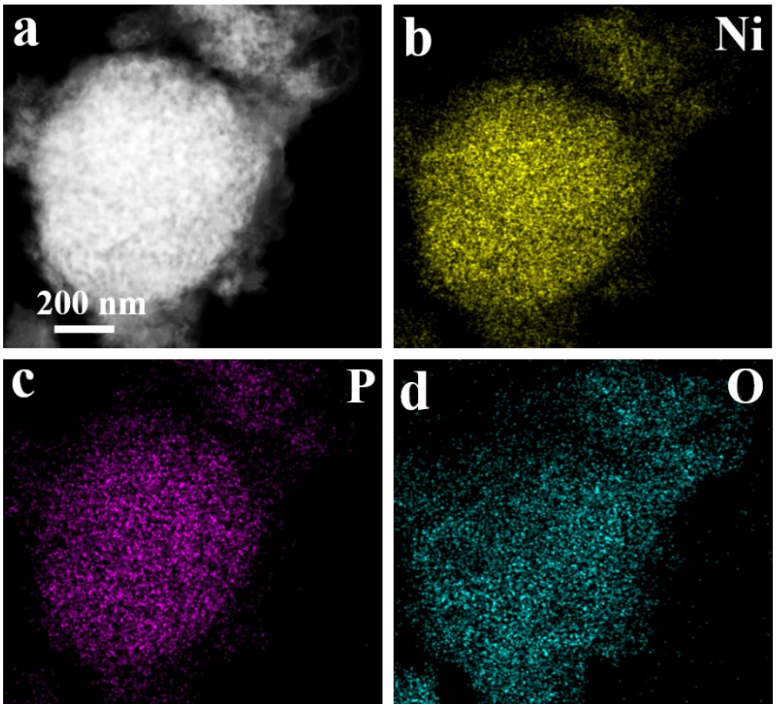

Fig. S15 HAADF-STEM image and corresponding elemental mapping images for P@Ni_2P-4 after HMFOR.